

## Ameliorative Potential of Polyphenolic Compounds in *Cucumis sativus* (Linn.) Fruit Pulp Extract on Streptozotocin-induced Diabetes in Male Wistar Rats

Olasunkanmi Kayode Awote<sup>1\*</sup>, Blessing Oluwaseun Ogunyinka<sup>1</sup>, Adesegun Gideon Adeyemo<sup>1</sup>, Olabisi Olufunmilayo Ogunrinola<sup>1</sup>, Ibrahim Oyeyemi Adenekan<sup>2</sup>, Babajide David Kayode<sup>3</sup>

<sup>1</sup> Department of Biochemistry, Lagos State University, PMB 0001, Ojo, Lagos State, Nigeria.

<sup>2</sup> Department of Mathematics, University of Louisiana at Lafayette, LA, United States of America.

<sup>3</sup> Department of Medical Biochemistry, Faculty of Basic Medical Sciences, Eko University of Medicine and Health Sciences, Badagry Expressway, Lagos State, Nigeria.

[olasunkanmi.awote@lasu.edu.ng](mailto:olasunkanmi.awote@lasu.edu.ng)

### Abstract

Diabetes mellitus continues to be a major global public health concern, underscoring the urgent need for continuous exploration of locally available medicinal plants and functional foods that are affordable, accessible, and capable of supporting effective management and improved health outcomes. This study investigated the effect of *Cucumis sativus* pulp extract (CSPE) on selected oxidative stress and diabetes-related biochemical indices. A total of 24 male Wistar rats were divided into 4 groups (n=6), including control, diabetic-untreated, and diabetic-treated groups (with CSPE or glibenclamide). Oxidative stress indices (hydrogen peroxide [H<sub>2</sub>O<sub>2</sub>], nitric oxide [NO], malondialdehyde [MDA], glutathione [GSH]); lipid profile (total cholesterol [TC], triglyceride [TRIG], high-density [HDL-Chol, low-density [LDL-Chol], and very-low-density [VLDL-Chol] lipoprotein cholesterol; liver antioxidant (superoxide dismutase [SOD], catalase [CAT]); and liver function (alanine [ALT], and aspartate [AST] aminotransferase) enzymes were evaluated using standard biochemical kits and procedures. PyRx and Biovia Discovery Studio were used for molecular docking studies, while SwissADME and ProTox were used to predict the ADME/T properties. Results showed that treatment with CSPE had a significant ( $p < 0.05$ ) increase in liver antioxidant enzymes, HDL-Chol, and GSH levels and a decrease in plasma ALT and AST, TC, TRIG, LDL-Chol, VLDL-Chol, H<sub>2</sub>O<sub>2</sub>, MDA, and NO compared to the diabetic-untreated group.  $\beta$ -sitosterol bound well with  $\alpha$ -amylase (-8.9 kcal/mol) and aldose reductase (-8.8 kcal/mol) while hesperidin bound to  $\alpha$ -glucosidase (-8.8 kcal/mol) and sorbitol dehydrogenase (-10.6 kcal/mol) with favorable ADME and toxicity profiles. In conclusion, CSPE can serve as a therapeutic agent in addition to its known nutritional properties in managing diabetes and its related complications.

**Keywords:** Diabetes mellitus, *Cucumis sativus* fruit, Phytochemistry, Polyphenols, Hypoglycemic, Hypolipidemic, Functional foods, Lipid profile, Hepatic function, Antioxidant.

### Introduction

Diabetes mellitus (DM) is one of the leading causes of death and morbidity worldwide, affecting people of all ages, genders, and geographic areas (Awote *et al.*, 2022; Popoviciu *et al.*, 2023). DM is a dangerous and chronic condition marked by consistently high blood glucose levels caused by insufficient insulin synthesis or the body's inability to use the generated insulin (Hossain *et al.* 2024). Nearly half of all adults with diabetes are unaware that they have the

disease, and an estimated 240 million adults worldwide live with undiagnosed diabetes (Magliano and Boyko, 2022). Meanwhile, 463 million adults have been estimated to be diagnosed with diabetes, which has been projected to increase to 578 and 700 million by the year 2030 and 2045, respectively (WHO, 2019; Awote *et al.*, 2023). DM has historically been linked to macrovascular problems, including peripheral artery disease, coronary heart disease, and stroke, as well as microvascular problems like diabetic kidney disease, retinopathy, and peripheral neuropathy (Kulkarni *et al.*, 2024).

The mitochondrial electron transport chain produces more free radicals in the form of reactive oxygen species (ROS) when blood glucose levels are elevated in diabetic patients (Mukai *et al.*, 2022). Excessive ROS and their accumulation, as well as the breakdown of antioxidant mechanisms inside cells or tissues, lead to oxidative stress (Afzal *et al.*, 2023). It has been suggested that this redox imbalance is a contributing factor to insulin resistance,  $\beta$ -cell malfunction, and impaired glucose intolerance, all of which can lead to type-2 diabetes (Andres *et al.*, 2023, Andres *et al.*, 2024).

Streptozotocin (STZ) is a naturally occurring alkylating antineoplastic drug that is especially harmful to the  $\beta$ -cell of the pancreas in mammals that produce insulin (Haghani *et al.*, 2022). Based on its structural similarity to glucose, STZ is injected intraperitoneally and enters pancreatic  $\beta$ -cells through glucose transporter 2 (GLUT2). Depending on the dose, STZ administration causes  $\beta$ -cell necrosis and subsequently a complete or partial loss of insulin production (Singh *et al.*, 2024).

Conventional antidiabetic drugs such as sulfonylureas, biguanides,  $\alpha$ -glucosidase inhibitors, agonists for peroxisome proliferator-activated receptor- $\gamma$  (PPAR $\gamma$ ), inhibitors of dipeptidyl peptidase IV (DPP IV), and inhibitors of sodium-glucose co-transporter-2 (SGLT2) are economical and the prolonged use of these medications has been associated with serious side effects including the risk of coma, edema, hypoglycemia, vomiting, bloating, possible weight gain, and issues with the central nervous and cardiovascular systems (Banu and Bhowmick, 2017, Daliri *et al.*, 2017, Padhi *et al.*, 2020). One of such antidiabetic drug is glibenclamide (glyburide). It is an oral sulfonylurea antidiabetic drug that lowers blood glucose by stimulating insulin secretion from pancreatic  $\beta$ -cells, primarily used in managing and/or treating type 2 diabetes mellitus. Therefore, to alleviate these side effects, new therapeutic approaches are required, and natural products have been reported as safe and natural alternatives (Yedjou *et al.*, 2023), including medicinal plants and fruits.

*Cucumis sativus* belongs to the *Cucurbitaceae* family and is commonly called “Cucumber” (Khan *et al.*, 2022). It is referred to as “Kukumba” amongst the Yoruba-speaking tribe of Southwestern Nigeria. Cucumbers are fruits with high water content and low calories, fat, cholesterol, and sodium (Adamu *et al.*, 2021). Numerous phytochemicals, including tannins, cardiac glycosides, phlobotannins, alkaloids, flavonoids, glycosides, steroids, terpenoids, carbohydrates, resins, saponins, and phytosterols, have been reported for the phytochemical screening of cucumber (Sari *et al.*, 2021). Flavonoids such as quercetin, apigenin, kaempferol, luteolin, lignans, and triterpenes; vitamins including biotin, vitamin B1, vitamin K, and pantothenic acid; minerals including copper, magnesium, potassium, manganese, and phosphorus have all been reported to be present in cucumber (Molly *et al.* 2017). The reported antimicrobial, antifungal, cytotoxic, antacid, carminative, hepato-protective, hypoglycemia, blood lipid-lowering, and hypo-lipidemic effects of cucumber have been associated with its embedded phytochemical constituent (Heidari *et al.* 2012).

Although several studies have explored the biological activities of *Cucumis sativus* (Linn.), there remains a noticeable gap in understanding its specific antioxidant-boosting, glucose-lowering, and lipid-modulating effects, particularly in streptozotocin-induced diabetes. Furthermore, limited research has integrated both experimental and computational methodologies to unravel or suggest the molecular mechanisms underlying the therapeutic potential of its active ingredients. Therefore, this study aims to comprehensively evaluate *C. sativus* by combining *in vivo* experiments with *in silico* analyses, offering novel insights into its role in managing diabetes and associated metabolic imbalances.

## Materials and Methods

### Plant Collection and Extraction

Fresh Cucumber (*Cucumis sativus*) was procured in March 2024 from a local market, Iyana-Iba market, Ojo, Lagos State, South-western Nigeria (Latitude: 6.4611° N and 3.2043° E) and identified by a botanist, Dr. K. T. Omolokun of the Department of Botany, Faculty of Science, Lagos State University, Ojo, Lagos State, Nigeria. Seven hundred (700) g of the fruit were rinsed under running water, peeled, and blended using a Kenwood blender (model No: KW505) to obtain a uniform pulp. The pulp was filtered using a muslin cloth, followed by Whatman no. 1 filter paper. The resultant liquid was concentrated under reduced pressure using a rotary evaporator to remove excess water, yielding 600 mg of concentrated cucumber pulp extract.

### Phytochemical Screening

The phytochemical components of *Cucumis sativus* were determined using the methods described by Awote *et al.* (2023). Alkaloids, flavonoids, phenols, saponins, steroids, tannins, terpenoids, and glycosides were identified, and the polyphenolics (total flavonoids, total phenolics, and total tannins) were quantified in mg/100g using a standard procedure and conditions.

### Gas Chromatography-Mass Spectroscopy (GC-MS) Analysis of *Cucumis sativus* Pulp Extract

An Agilent 5977B GC/MSD system with an Agilent 8860 auto-sampler, a gas chromatograph interfaced to a mass spectrometer (GC-MS) equipped with an Elite-5MS (5% diphenyl/95% dimethyl polysiloxane) fused a capillary column (30 × 0.25µm ID × 0.25µm df) were used to perform the GC-MS analysis of the extract. An electron ionization device with an ionization energy of 70 eV was used in electron impact mode for GC-MS detection. A split ratio of 10:1 was used with an injection volume of 1µL and helium gas (99.999%) as the carrier gas at a steady flow rate of 1 mL/min. To calibrate the GC-MS, five (5) point serial dilution calibration standards (1.25, 2.5, 5.0, and 10.0 ppm) were made from the 40 ppm stock solution. Temperatures were maintained at 300 °C for the injector, 250 °C for the ion source, and 100 °C (isothermal) for 0.5 min in the oven, with a 20 °C/min increase to 280 °C (2.5 min) for the oven. Mass spectra were obtained at 70 eV with a 0.5 s scanning interval and fragments ranging from 45 to 450 Da. GC/MS ran for a total of 21.33 minutes, with a solvent delay of 0 to 3 minutes (Awote *et al.*, 2024).

### High-Performance Liquid Chromatography (HPLC) Analysis of *C. sativus* Pulp Extract.

The measurement of flavonoid components in the extracts was carried out using high-performance liquid chromatography (HPLC) on an HPLC-Agilent Technologies 1200 series

liquid chromatograph equipped with a UV detector. A Hypersil BDS C18 column (150 × 4.6 mm, 5 µm particle size) prepacked for the reversed-phase was used for the chromatography, which was carried out at 250°C. A (0.1% formic acid in water) and B (HPLC grade acetonitrile) are combined to generate the mobile phase, which has a steady flow rate of 0.75 mL/min. At 0 min, 94% A, 14 min, 83.5% A, 16 min, 83% A, 18 min, 82.5% A, 20 min, 82.5%; 22–24 min, 81.5%; and 27–40 min, 80% A, the linear gradient solvent system began. The detection wavelength was 280 nm (Awote *et al.*, 2024).

### ***In-silico* Studies Ligand Modeling**

The GC-MS and HPLC-generated ligands' 3D crystal structures were downloaded in sdf format from the PubChem database (<https://pubchem.ncbi.nlm.nih.gov/>). Also, the ligands' canonical SMILES were downloaded from the PubChem database. Biovia Discovery Studios 2021 was used to convert the ligands to .pdb format, and Open Babel (<https://openbabel.readthedocs.io/en/latest/Forcefields/mmff94.html>) was utilized in optimizing the energy of the ligand molecules. Following energy minimization, the ligand molecules were converted specifically into pdbqt AutoDock ligand format (Awote *et al.*, 2024).

### **Protein (Target) Preparation**

The selected protein targets were sourced from the Protein Data Bank (<https://www.rcsb.org>) and a deposited crystal structure of *Homo sapiens* was used as a reference to model the 3D structures of these proteins. The protein grid box coordinates were set at x= 8.689, y= -27.9742, and z= 15.7172; x= -12.1777, y= -35.4768, and z= 88.7572; x= 80.183, y= 62.3450, and z= 3.4609; and x= -0.3408, y= -0.6404, and z= 15.0471 for human pancreatic α-amylase (PDB ID: 2QMK), human pancreatic α-glucosidase (PDB ID: 5NN8), human pancreatic sorbitol dehydrogenase (PDB ID: 1PL6), and aldose reductase (PDB ID: 3S3G), respectively, to target the active sites of each protein. Biovia Discovery Studio 2021 was used to eliminate heteroatoms, ligand groups, and water molecules from the protein structures and add hydrogen polar to protein structures to prepare them for molecular docking analysis (Awote *et al.*, 2024).

### **Molecular Docking**

The AutoDock Vina tool was utilized for molecular docking studies. The usual diabetes standard drugs, acarbose and tolrestat, and the co-crystallized ligands for the target proteins were utilized. Following the sorting of the ligand molecules according to increasing binding energies, the investigation was based on binding free energy values (Awote *et al.*, 2024).

### **Absorption, Distribution, Metabolism, Excretion & Toxicity (ADMET) Properties Prediction**

Based on binding energy, the top ten ligands were selected, and their drug-likeness parameters, physicochemical properties, pharmacokinetic properties, lipophilicity, water solubility, medicinal chemistry, and toxicity were predicted using SwissADME and admetSAR. These predictive algorithms were used to evaluate the ligands' general eligibility as possible drug candidates and to offer information about their possible safety, pharmacological characteristics, and therapeutic efficacy (Awote *et al.*, 2024).

## Experimental Animals

Twenty-four (24) male Wistar rats (8 weeks old), with an average weight of 103 g (range of 100–105 g), were sourced from the animal house of the Department of Biochemistry, Faculty of Science, Lagos State University, Nigeria. The rats were kept in regular day/night cycles while they were made to have access to clean drinking water and commercial pelleted feed (Vital feed® Nigeria). Current national and international criteria were followed in the care and usage of the Wistar rats during the study. With the ethical approval number LASU/23/REC/055, the Lagos State University Research Ethics Committee authorized the study procedure.

## Induction of Type-2 Diabetes mellitus

Type-2 Diabetes Mellitus (T2DM) was introduced into the overnight fasted rats intraperitoneally at a dose of 60 mg/kg body weight of Streptozotocin (STZ) (Sigma-Aldrich Chemicals Company, St. Louis, MO., U.S.A.) dissolved in freshly prepared 0.1 M of iced-cold citrate buffer (pH 4.5) (Ogunyinka *et al.*, 2017). To prevent hypoglycemia, the rats were maintained with 20% glucose (Unique Pharmaceuticals, Sango Otta, Ogun State, Nigeria) for six hours following the induction and later with 5% glucose for the following 24 hours (Prince and Menon, 2003). On the third day (72 hours) after induction, hyperglycemia was found to be gradually developing, but by the seventh day, all of the rats had stabilized and were consistently hyperglycemic. The rats exhibiting a fasting blood glucose level of 200 mg/dL or higher by the seventh day were classified as diabetic and included in the investigation. The fourth day after STZ induction marked the start of the treatments, which lasted for 28 days. The blood glucose concentrations were measured after drawing blood from the rats' tails using an Accu-Check glucometer. The success rate of induction exceeded 76.9%.

## Animal Groupings and Treatments

Animal groupings and treatment were carried out using the modified method of Ogunyinka *et al.* (2017). Before this study, the rats were fasted overnight and divided into four (4) groups (A–D) of six rats each, randomly selected so that the group mean weights were the same.

Group A (normal control) consisted of non-diabetic rats that received 2 mL/kg body weight/day of distilled water orally for 28 days.

Group B (positive control) = streptozotocin (STZ)-induced diabetic rats orally administered 2 mL/kg body weight/ day distilled water for 28 days.

Group C = diabetic rats orally administered 600 mg/kg body weight/ day of *C. sativus* pulp extract for 28 days.

Group D = diabetic rats orally administered 5 mg/kg body weight/ day of glibenclamide (®Daonil, Hoechst Marion Roussel Limited, Mumbai, India) for 28 days.

## Blood Collection

After receiving medication for 28 days, each rat was given an injection of 0.2 mL of ketamine to induce anesthesia and then dissected. The gradual lack of corneal and pedal responses confirmed anesthesia. Afterward, a sterile 21 G needle placed on a 5 mL plunger syringe (®Cliniject Hypodermic Syringe, Albert David Limited, Mandideep-462046, Raisen District, India) was used to collect fresh blood from the heart chamber and stored in plain sample bottles. The blood was centrifuged immediately for 15 minutes at 2500 rpm. The supernatant (serum)

was then removed and stored in the refrigerator until required for biochemical analysis.

## **Biochemical Assays**

The effects of *Cucumis sativus* pulp extracts on STZ-induced diabetic Wistar rats were evaluated using the following biochemical parameters:

### **Protein Determination**

The protein concentration of the various samples was determined using the Lowry method as described by Lowry *et al.* (1951) with a few modifications. In summary, 400  $\mu\text{L}$  of solution C (200  $\mu\text{L}$  solution B (1% copper sulfate ( $\text{CuSO}_4 \cdot 5\text{H}_2\text{O}$ ) and 2% sodium potassium tartrate) and

9.8 mL of solution A (0.1 M sodium hydroxide and 2% sodium bicarbonate), 40  $\mu\text{L}$  of folin C, and 25  $\mu\text{L}$  of each sample were mixed with 0.5 mg/mL bovine serum albumin (BSA). After thoroughly mixing, the mixture was left to stand. At 650 nm, the absorbance was measured against a blank that contained 60  $\mu\text{l}$  of solution C, water, or buffer. From the Lowry standard curve, the protein concentrations of each group were extrapolated and expressed in mg/mL.

### **Catalase (CAT) Activity**

Catalase activity was determined according to the method of Oladimeji *et al.* (2022). In summary, 10  $\mu\text{L}$  of the homogenate and 590  $\mu\text{L}$  of hydrogen peroxide (590  $\mu\text{L}$  of 19 mM solution) were pipetted into a 1 cm quartz cuvette. The mixture was quickly swirled to mix it thoroughly, and it was then put in a spectrophotometer. The change in absorbance was measured at 240 nm for 10 seconds for 2 minutes. The extinction coefficient of hydrogen peroxide, which is 240 nm, was used to express catalase activity as  $\mu\text{mol}/\text{mg}$  protein.

### **Superoxide Dismutase (SOD) Activity**

SOD activity was determined by the Epinephrine method reported by Oladimeji *et al.* (2023). In brief, 2.5 mL of 0.05 M phosphate buffer (pH 7.8) was mixed with 0.1 mL of the tissue homogenate supernatant. At the point of absorbance measurement, which was measured at 750 nm for one minute and thirty seconds at intervals of 15 seconds, 0.3 mL of adrenaline solution (0.059%) was then added. After calculation, SOD activity was then expressed as mmol/mg protein.

### **Lipid Profile Estimation**

Using standard diagnostic test kits (Randox Laboratories, Crumlin, U.K.), the lipid profile (triglyceride (TG), total cholesterol (TC), and high-density lipoprotein cholesterol (HDL-c)) of the treated Wistar rats was analyzed in the serum sample. The Friedewald formula was used to determine serum low-density lipoprotein cholesterol (LDL-c) and very-low-density lipoprotein cholesterol (VLDL-c):  $\text{LDL-c} = [\text{TC} - (\text{HDL-c} + \text{TG}/5)]$ , and  $\text{VLDL-c} = \text{TAG}/5$ , respectively (Awote *et al.*, 2021).

### **Non-Protein Thiol (GSH) Estimation**

The level of reduced glutathione (GSH) was estimated according to Jollow *et al.* (1974). Using Ellman's reagent (DTNB), the glutathione (GSH) content was determined calorimetrically. Sulfa-salicylic (4%) was added to the supernatant in a 1:1 ratio to precipitate it. After being stored at 4°C for one hour, the samples were centrifuged for ten minutes at 4°C at 5000 rpm.

Phosphate buffer (0.1 M, 550  $\mu$ L), 100  $\mu$ L of supernatant, and 100  $\mu$ L of DTNB were mixed to make up the assay combination. The absorbance was read at 412 nm, and the results were expressed as  $\mu$ mol of GSH/mg protein.

### **Nitric Oxide (NO) Estimation**

After the Griess reaction, the concentrations of nitrite in serum or supernatants were determined by incubating 250  $\mu$ L of the homogenate with 250  $\mu$ L of Griess reagent at room temperature for 20 minutes. The spectrophotometric method was used to measure the absorbance at 550 nm. The absorbance of a standard solution containing known amounts of sodium nitrite was compared to determine the nitrite content; the findings were expressed as mmol/L (Green *et al.*, 1983).

### **Hydrogen Peroxide (H<sub>2</sub>O<sub>2</sub>) Estimation**

In summary, FOX was formed by adding 10 mL of Xylenol, 10 mL of sorbitol, and 50 mL of ammonium ferrous sulfate to 30 mL of distilled water. In the meantime, 10  $\mu$ L of homogenate and 290  $\mu$ L of FOX were well mixed by vortexing until foamy. After 30 minutes of room temperature incubation, a faint pink color complex is produced. At a wavelength of 560 nm, the absorbance was measured against a blank (distilled water). The hydrogen peroxide generated was calculated and expressed in mmol/mL (Wolff, 1994).

### **Lipid Peroxidation Estimation**

Lipid peroxidation was determined by measuring the formation of thiobarbituric acid reactive substance (TBARS) according to the method of Varshney and Kale, (1990). Briefly, tissue samples were homogenized in 0.1 M phosphate buffer (pH 7.4) in a ratio of 1:5. 200  $\mu$ L of the stock reagent—an equal volume of trichloroacetic acid (10%, w/v) and 2-thiobarbituric acid (0.75%, w/v) in 0.1 M HCl was added to 100  $\mu$ L of homogenate, and the mixture was incubated at 95°C for an hour using a water bath. After cooling, the solution was centrifuged at 3000 rpm for 10 minutes, and the absorbance of the supernatant was measured at 532 nm and 600 nm. Lipid peroxidation was expressed as nmol.

### **Determination of Enzymatic Activities**

Using commercial diagnostic kits (Randox, U.K.), the activities of alanine transaminase (ALT, EC 2.6.1.2) and aspartate transaminase (AST, EC 2.6.1.1) were measured following the manufacturer's instructions (Fagbohun *et al.*, 2020). At 340 nm, each enzyme's activity was determined using a spectrophotometer.

### **Statistical Analysis**

The results are presented as Mean  $\pm$  Standard Error of Mean (SEM). For the descriptive statistics, One-way ANOVA was used to compare the treated and control groups using GraphPad Prism 5.0 (GraphPad Prism Software Inc., San Diego, CA, USA). When comparing the treated and control groups, statistically significant differences were identified at  $p < 0.05$  with a 95% confidence interval. When significant, means were separated using the Bonferroni post-hoc test.

## Results

Table 1 shows the preliminary phytochemical screening of *Cucumis sativus* pulp extract (CSPE). The qualitative analysis shows the presence of alkaloids, flavonoids, phenols, saponins, tannins, steroids, terpenoids, and glycosides. Furthermore, the polyphenolic quantitative analysis showed that CSPE contained abundant flavonoids, followed by phenolic acids and tannins. Table 2 –3 shows the comprehensive phytochemical screening of CSPE.

Eleven (11) polyphenolic compounds and forty-one (41) secondary metabolites were observed from the HPLC and GC-MS analyses of CSPE, respectively. The GC-MS analysis showed a 99.94 area percentage.

**Table 1.** Preliminary Phytochemical Profile of *Cucumis sativus* Pulp Extract

SN	Phytochemicals	Qualitative	Polyphenolic content
1	Alkaloids	+	NQ
2	Flavonoids	+	41.8 ± 0.88 (mg QE/ 100g)
3	Phenolics	+	59.4 ± 0.87 (mg GAE/ 100g)
4	Saponins	+	NQ
5	Steroids	+	NQ
6	Tannins	+	45.5 ± 0.11 (mg GAE/ 100g)
7	Terpenoids	+	NQ
8.	Glycosides	+	NQ

**KEY:** - = Absent, + = Present, NQ= not quantified, QE= milligrams of quercetin equivalents per 100g extract, GAE= milligrams of gallic acid equivalents per 100g extract

**Table 2.** HPLC profile of the bioactive compounds present in *Cucumis sativus* pulp extract

SN	Compounds	MW (g/mol)	MF	Conc. (ppm)	Class of Compound
1	Caffeic acid	180.16	C <sub>9</sub> H <sub>8</sub> O <sub>4</sub>	0.30	Phenolic acid
2	Chlorogenic acid	354.31	C <sub>16</sub> H <sub>18</sub> O <sub>9</sub>	0.69	Phenolic acid
3	Epigallocatechin	306.21	C <sub>15</sub> H <sub>14</sub> O <sub>7</sub>	0.2	Flavonoid
4	Gallic acid	170.12	C <sub>7</sub> H <sub>6</sub> O <sub>5</sub>	0.48	Phenolic acid
5	Hesperidin	610.56	C <sub>28</sub> H <sub>34</sub> O <sub>15</sub>	0.34	Flavonoid glycoside
6	Kaempferol	286.24	C <sub>15</sub> H <sub>10</sub> O <sub>6</sub>	1.76	Flavonoid
7	Protocatechuic acid	154.12	C <sub>7</sub> H <sub>6</sub> O <sub>4</sub>	0.87	Phenolic acid

8	Rutin	610.52	C <sub>27</sub> H <sub>30</sub> O <sub>16</sub>	0.65	Flavonoid glycoside
9	Tannic acid	1701.2	C <sub>76</sub> H <sub>52</sub> O <sub>46</sub>	2.58	Tannins
10	Vannilic acid	168.15	C <sub>8</sub> H <sub>8</sub> O <sub>4</sub>	1.67	Phenolic acid
11	Vitexin	432.4	C <sub>21</sub> H <sub>20</sub> O <sub>10</sub>	0.56	Flavonoid glycoside

**Table 3.** GC-MS profile of bioactive compounds present in *Cucumis sativus* pulp extract

SN	Compounds	MW	MF	RT	Area (%)	Class of compounds
1.	3'-Benzyloxy-5,6,7,4'-tetramethoxyflavone	448.46	C <sub>26</sub> H <sub>24</sub> O <sub>7</sub>	9.83	0.64	Flavonoids
2.	3-Feruloylquinic Acid	368.34	C <sub>17</sub> H <sub>20</sub> O <sub>9</sub>	6.89	3.10	Phenolic acid
3.	3-Methyl-L-histidine	169.18	C <sub>7</sub> H <sub>11</sub> N <sub>3</sub> O <sub>2</sub>	5.4	4.61	Alkaloid
4.	3-p-Coumaroylquinic Acid	338.31	C <sub>16</sub> H <sub>18</sub> O <sub>8</sub>	7.12	4.20	Phenolic acid
5.	5,7-dimethoxyflavone	282.29	C <sub>17</sub> H <sub>14</sub> O <sub>4</sub>	10.25	1.31	Flavonoid
6.	5-Aminolevulinic acid	131.13	C <sub>5</sub> H <sub>9</sub> NO <sub>3</sub>	5.12	2.13	Amino acid derivative
7.	5-hydroxyisovanillic acid	184.15	C <sub>8</sub> H <sub>8</sub> O <sub>5</sub>	11.59	1.15	Phenolic acid
8.	6-Octadecenoic acid (Z)	282.5	C <sub>18</sub> H <sub>34</sub> O <sub>2</sub>	12.08	0.46	Fatty acid
9.	9,12-Octadecadienoic acid (Z,Z)-, methyl ester	294.5	C <sub>18</sub> H <sub>32</sub> O <sub>2</sub>	54.89	6.91	Fatty acid ester
10.	9-Octadecenoic acid, methyl ester	296.5	C <sub>19</sub> H <sub>36</sub> O <sub>2</sub>	55.03	4.16	Fatty acid ester
11.	10-Octadecenoic acid, methyl ester	296.5	C <sub>19</sub> H <sub>36</sub> O <sub>2</sub>	55.15	8.41	Fatty acid ester
12.	Arachidic acid	312.5	C <sub>20</sub> H <sub>40</sub> O <sub>2</sub>	11.85	1.42	Fatty acid
13.	β-sitosterol	414.71	C <sub>29</sub> H <sub>50</sub> O	17.6	0.59	Sterol
14.	Catechin	290.27	C <sub>15</sub> H <sub>14</sub> O <sub>6</sub>	8.45	2.10	Flavonoid
15.	Coumaric acid	146.14	C <sub>9</sub> H <sub>6</sub> O <sub>2</sub>	4.78	1.80	Phenolic compound
16.	Dodecanoic	200.32	C <sub>12</sub> H <sub>24</sub> O <sub>2</sub>	8.72	9.95	Fatty acid
17.	Fluconazole	306.27	C <sub>13</sub> H <sub>12</sub> F <sub>2</sub> N <sub>6</sub> O	56.03	5.15	Synthetic compound
18.	Galactinol	342.3	C <sub>12</sub> H <sub>22</sub> O <sub>11</sub>	3.91	0.90	Carbohydrate
19.	Genkwanin	284.26	C <sub>16</sub> H <sub>12</sub> O <sub>5</sub>	16.04	5.93	Flavonoid
20.	Gitoxigenin	390.5	C <sub>23</sub> H <sub>34</sub> O <sub>5</sub>	13.5	1.17	Cardiac glycoside
21.	Hexadecanoic acid, methyl ester	270.5	C <sub>17</sub> H <sub>34</sub> O <sub>2</sub>	49.48	3.23	Fatty acid ester
22.	Hexa-Hydro-farnesol	228.41	C <sub>15</sub> H <sub>32</sub> O	20.24	0.56	Terpenoid
23.	Hexamethylinositol	264.31	C <sub>12</sub> H <sub>24</sub> O <sub>6</sub>	8.3	0.90	Inositol derivative
24.	Hydroquinine	326.4	C <sub>20</sub> H <sub>26</sub> N <sub>2</sub> O <sub>2</sub>	13.57	0.70	Alkaloid
25.	Inosine-1-methyl	282.25	C <sub>11</sub> H <sub>14</sub> N <sub>4</sub> O <sub>5</sub>	18.17	0.68	Nucleoside derivative
26.	Isolongifolol	222.37	C <sub>15</sub> H <sub>26</sub> O	15.78	1.75	Terpenoid

SN	Compounds	MW	MF	RT	Area (%)	Class of compounds
27.	Isomyristic	228.37	C <sub>14</sub> H <sub>28</sub> O <sub>2</sub>	11.44	1.12	Fatty acid
28.	Kaempferitrin	578.52	C <sub>27</sub> H <sub>3</sub> O <sub>14</sub>	5.23	2.10	Flavonoid glycoside
29.	L-Arginine	174.2	C <sub>6</sub> H <sub>14</sub> N <sub>4</sub> O <sub>2</sub>	5.58	1.71	Amino acid
30.	Linoleic acid	280.4	C <sub>18</sub> H <sub>32</sub> O <sub>2</sub>	15.8	0.45	Fatty acid
31.	Linoleic acid ethyl ester	308.5	C <sub>20</sub> H <sub>36</sub> O <sub>2</sub>	56.76	1.97	Fatty acid ester
32.	L-Lysine	146.19	C <sub>6</sub> H <sub>14</sub> N <sub>2</sub> O <sub>2</sub>	6.22	1.59	Amino acid
33.	Mangiferin	422.3	C <sub>19</sub> H <sub>18</sub> O <sub>11</sub>	10.045	0.51	Phenolic compound
34.	Melibiose	342.3	C <sub>12</sub> H <sub>22</sub> O <sub>11</sub>	6.39	2.09	Disaccharide
35.	Methyl-6,7-dimethoxycoumarin -4-acetate	278.26	C <sub>14</sub> H <sub>14</sub> O <sub>6</sub>	10.799	0.52	Coumarin derivative
36.	Octadecanoic acid methyl ester	298.5	C <sub>19</sub> H <sub>38</sub> O <sub>2</sub>	39.13	5.97	Fatty acid ester
37.	Phytol	296.5	C <sub>20</sub> H <sub>40</sub> O	14.05	0.91	Diterpenoid
38.	Prunin Naringenin-7-O-Glucoside	434.39	C <sub>21</sub> H <sub>22</sub> O <sub>10</sub>	6.45	3.50	Flavonoid glycoside
39.	Quercetin-3,5,7,3',4'-pentamethyl ether	372.4	C <sub>20</sub> H <sub>20</sub> O <sub>7</sub>	21.3	0.47	Flavonoid
40.	Stevioside	804.9	C <sub>38</sub> H <sub>60</sub> O <sub>18</sub>	7.1	0.87	Glycoside
41.	Vincadiformine	338.4	C <sub>21</sub> H <sub>26</sub> N <sub>2</sub> O <sub>2</sub>	9.7	4.05	Alkaloid

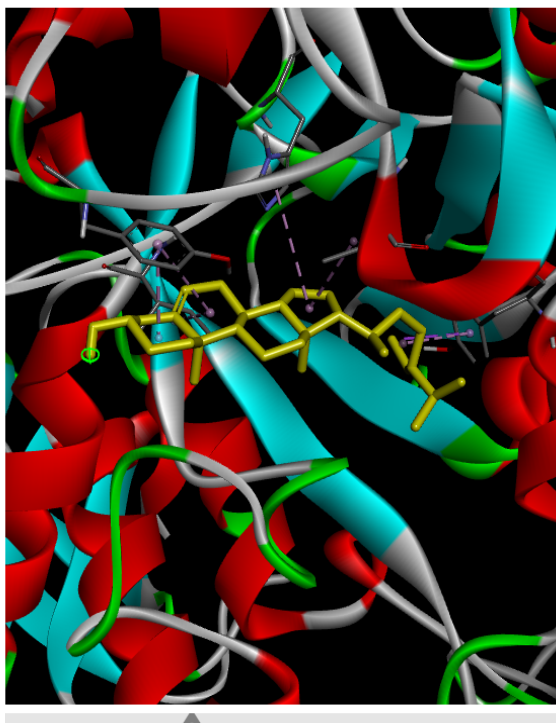
MW = Molecular weight (in g/mol), MF = Molecular formula, and RT = Retention time

Figure 1A shows the complex interaction between  $\beta$ -Sitosterol, the ligand with the best binding affinity with human  $\alpha$ -amylase protein. The 2D structure illustrates the formation of a pi-sigma bond between the ligand and Tyr62 (amino acid) at the surface of the protein. Additionally, Leu162, His201, Tyr151, and Ile235 formed both alkyl and pi-alkyl bonds with  $\beta$ -Sitosterol. Meanwhile, Glu240, Thr163, His299, Asp197, Arg195, His305, Asp300, Trp58, Trp59, Leu165, Ala198, Glu233 and Lys200 formed van der Waals interaction with  $\beta$ -Sitosterol.

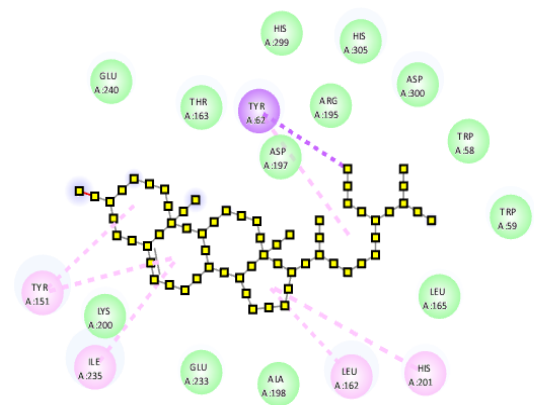
Figure 1B shows the 3D and 2D structures of hesperidin (ligand) – human  $\alpha$ -glucosidase (protein) complex interaction. Arg591, Thr593, Arg837, His432, Trp859, and Asp860 formed conventional hydrogen bonds; Glu863 formed an unfavorable acceptor-acceptor interaction; Asp513, Arg591, and Arg437 formed pi-cation and pi-anion interactions while His507 and Arg591 both formed pi-alkyl and alkyl bonds. Additionally, Pro511, Arg436, Leu899, Glu895, Asp861, Gly862, Tyr366, and Thr834 formed van der Waals interactions with hesperidin. Hesperidin (ligand) also formed a complex with sorbitol dehydrogenase (protein). Here in, Cys249, Arg208, Arg298, and Thr121 formed conventional hydrogen bonds while, Gly179, Asp203, Gly181, Ile56, Phe297, Phe59, Pro122, Tyr50, Phe118, Leu274, Ser46, Val296, Val272, His49, Val159, Ile183, Gly45 and Thr250 formed van der Waals interaction with hesperidin (Figure 1C).

Figure 1D shows the complex interaction between  $\beta$ -Sitosterol (ligand) and human aldose reductase (protein). The 2D structure illustrates the formation of pi-alkyl and alkyl interactions between the best-fitting ligand and Cys298, Tyr48, His110, Trp219, Phe122, and Trp20 (amino acids) at the surface of the protein. Meanwhile, Tyr209 and Trp20 formed pi-sigma interaction. Additionally, Ser302, Leu301, Leu300, Trp79, Asn160, Ser159, Trp111, Lys77, Gln183,

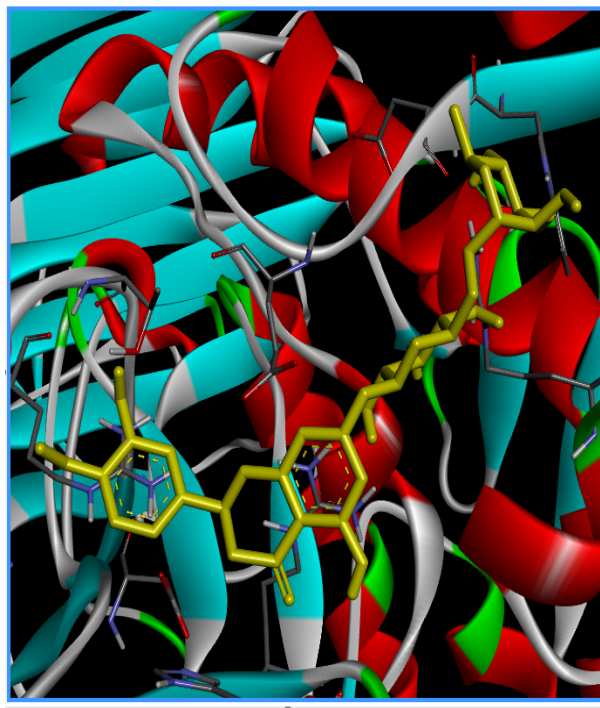
Asp43, Ile260 and Ser210 formed van der Waals interaction with  $\beta$ -Sitosterol.



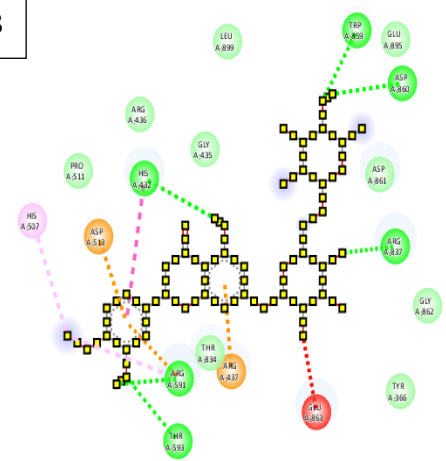
**A**



- Interactions**
- van der Waals
  - Pi-Sigma
  - Alkyl
  - Pi-Alkyl



**B**



- Interactions**
- van der Waals
  - Conventional Hydrogen Bond
  - Unfavorable Acceptor-Acceptor
  - Pi-Cation
  - Pi-Anion
  - Pi-Pi T-shaped
  - Alkyl
  - Pi-Alkyl

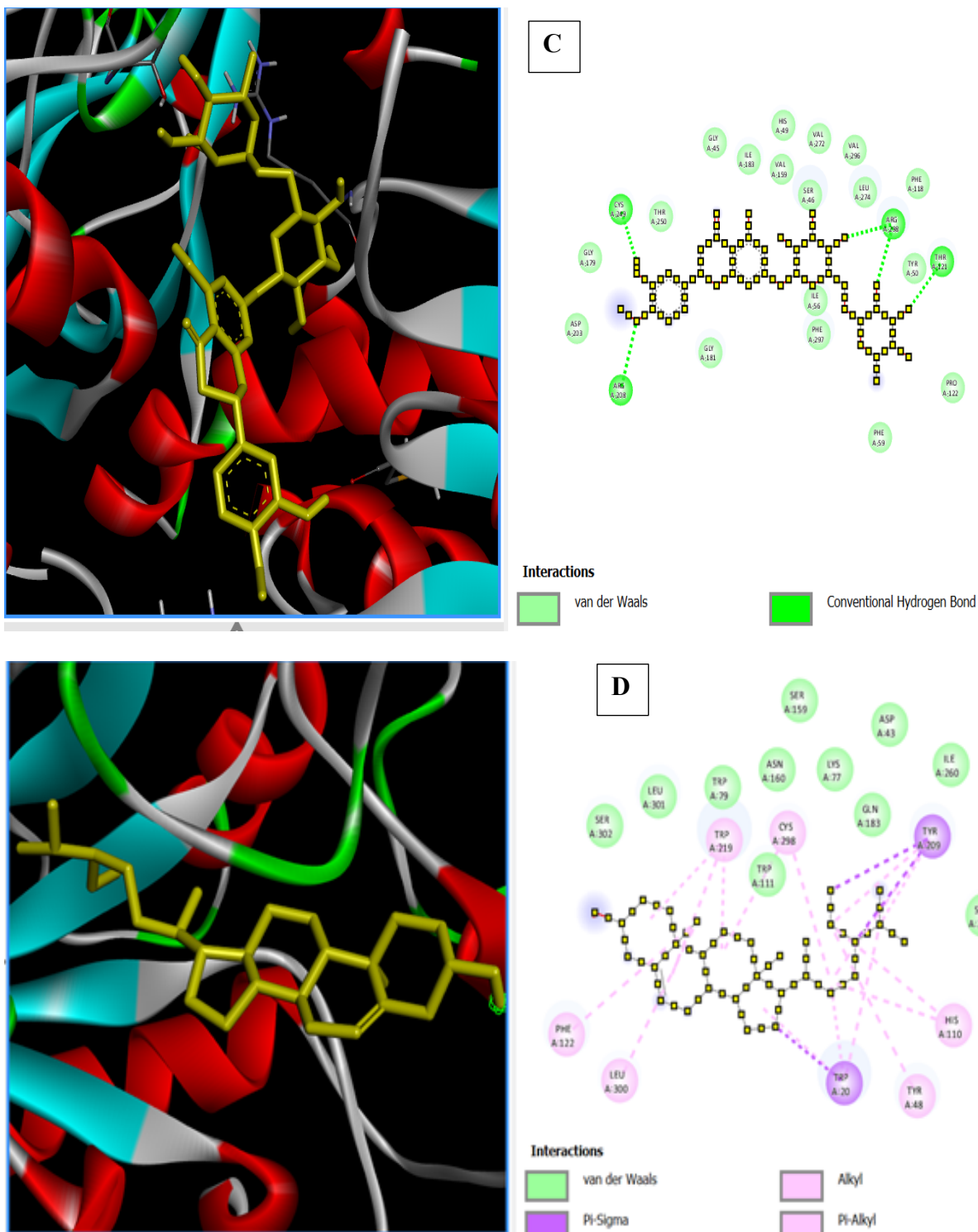


**Figure 1.** Interaction of (a)  $\beta$ -sitosterol (b) hesperidin (c) hesperidin (d)  $\beta$ -Sitosterol with the active site amino acids of human pancreatic  $\alpha$ -Amylase (PDB ID: 2QMK),  $\alpha$ -glucosidase (PDB ID: 5NN8), human sorbitol dehydrogenase (PDB ID: 1PL6), and human aldose reductase (PDB ID: 3S3G) shown in 3D (left) and 2D (right) structures.

Table 4 shows the top ten (10) ligands based on their binding affinities. Better ligands and binding affinities result from reduced binding energies. All these 10 ligands showed a better binding affinity with either of the carbohydrate metabolizing enzymes compared to the standard drugs, acarbose, and tolrestat. Here,  $\beta$ -Sitosterol, a molecule from the extract of *Cucumis sativus*, showed a better binding energy of -10.6 kcal/mol and thus better binding affinity

compared to the standard drugs used in this study. Additionally, all the top ten ligands showed a better binding affinity with  $\alpha$ -amylase and  $\alpha$ -glucosidase compared to acarbose, except for 3-Feruloylquinic acid (-6.7 kcal/ mol in  $\alpha$ -glucosidase). Furthermore, all the top ten ligands showed a better binding affinity with sorbitol dehydrogenase and aldose reductase compared to the tolrestat, except for 3-Feruloylquinic acid (-6.7 kcal/ mol) and chlorogenic acid (-5.5 kcal/ mol) in sorbitol dehydrogenase.

**Table 4.** Binding Energies (Kcal/ mol) of the top ten (10) ligands.

No	Ligands	PubChem ID	Diabetes Protein Targets (kcal/mol)			
			$\alpha$ -Amylase	$\alpha$ -Glucosidase	Sorbitol Dehydrogenase	Aldose Reductase
1	$\beta$ -Sitosterol	222284	<b>-8.9</b>	-7.7	-8.4	<b>-10.6</b>
2	Genkwanin	5281617	-6.9	-7.1	-7.4	-9.9
3	Epigallocatechin	72277	-6.9	-7.3	-7.6	-9.7
4	Hesperidin	10621	-7.8	<b>-8.8</b>	<b>-8.8</b>	-9.6
5	Chlorogenic acid	1794427	-8.0	-7.0	-6.7	-9.6
6	Rutin	5280805	-7.5	-8.5	-8.3	-9.6
7	Prunin-Naringenin-7-O-glucosides	92794	-8.8	-8.3	-8.6	-9.5
8	3'-Benzyloxy-5,6,7,4'-tetramethoxyflavone	7020621	-7.6	-8.0	-8.6	-9.4
9	3-Feruloylquinic acid	10133609	-7.8	-6.7	-5.5	-9.3
10	Kaempferitrin	5486199	-7.5	-8.5	-8.6	-9.3
11	Tolrestat*	53359	-	-	-7.0	-7.7
12	Acarbose *	41774	-6.8	-7.2	-	-

**KEY:** \* denotes the standard drugs incorporated in this study

Tables 5.1 – 5.6 show the absorption, distribution, metabolism, excretion, and toxicity (ADMET) properties of the top ten (10) ligands and the standard drugs, acarbose and tolrestat.

Table 5.1 illustrates the physicochemical properties and  $\beta$ -Sitosterol, genkwanin, epigallocatechin, chlorogenic acid, prunin-naringenin-7-O-glucosides, 3'-benzyloxy-5,6,7,4'-tetramethoxy flavone, and 3-feruloylquinic acid obeyed the Lipinski rule of five while hesperidin, rutin, and kaempferitrin disobeyed it. The Lipinski rule of five (RO5) states that a molecule has an increased chance of being druggable if it has no more than two violations of the following demands: molecular weight less than 500, log P less than 5, hydrogen bond donors

less than 5, hydrogen bond acceptors less than 10, and rotatable bonds less than 10.

Table 5.2 shows lipophilicity and water solubility predictions of the top ten ligands. With a value of 5.05, the ligand with the highest binding affinity,  $\beta$ -Sitosterol, displayed the best logarithm of the partition coefficient (Log P). All ligands except  $\beta$ -Sitosterol are predicted to be either moderately soluble, soluble, or very soluble.

The pharmacokinetic properties showed in Table 5.3 showed that, of the top ten ligands, only four ligands- genkwanin, epigallocatechin, 3'-benzyloxy-5,6,7,4'-tetramethoxy flavone, and acarbose have high gastrointestinal absorption. In addition, none of the ligands demonstrated positive blood-brain barrier permeability while only five of these top ten ligands were found to be a p-glycoprotein substrate. One of the best ten ligands namely 3'-benzyloxy-5,6,7,4'-tetramethoxy flavone and a standard drug tolrestat were predicted to be CYP2C19 inhibitors. Concurrently, it was discovered that genkwanin and tolrestat are inhibitors of CYP1A2 while genkwanin is the sole inhibitor of CYP2D6. Moreover, genkwanin and 3'-Benzyloxy-5,6,7,4'-tetramethoxy flavone were identified as CYP2C9 and CYP3A4 inhibitors.

Table 5.4 shows the drug-likeness properties of the top ligands with a good bio-availability score range of 0.11 – 0.55. This shows that the top ten ligands have a good drug-likeness property since a minimum of 0.10 bioavailability score is required of a compound to be considered as a drug candidate. Table 5.5 shows the medicinal chemistry properties. Here, three of the top ten ligands – epigallocatechin, chlorogenic acid, and rutin showed indications for positive pan-assay interference compounds (PAINS). Meanwhile, genkwanin and epigallocatechin showed lead-likeness indication. Furthermore, the top ten ligands and the standard drugs showed a good synthetic accessibility score range of 2.34 to 7.34.

The top ten ligands showed a negative and positive indicator for carcinogenic and reproductive toxicity, respectively. The standard drugs and five of the top ligands including,  $\beta$ -sitosterol, epigallocatechin, chlorogenic acid, rutin, and 3-feruloyl quinic acid showed positive indicators for hepatic and respiratory toxicity. Additionally,  $\beta$ -sitosterol, epigallocatechin, chlorogenic acid, prunin-naringenin-7-O-glucosides, acarbose, tolrestat and 3-feruloyl quinic acid predicted mitochondria toxicity while prunin-naringenin-7-O-glucosides predicted nephrotoxicity (Table 5.6).

**Table 5.1.** Physicochemical properties of the top ten ligands

S/N	Ligands	PubChem ID	MF	MW(g/mol)	NRB	NHBA	NHBD
1	$\beta$ -Sitosterol	222284	C <sub>29</sub> H <sub>50</sub> O	414.71	6	1	1
2	Genkwanin	5281617	C <sub>16</sub> H <sub>12</sub> O <sub>5</sub>	284.26	2	5	2
3	Epigallocatechin	72277	C <sub>15</sub> H <sub>14</sub> O <sub>7</sub>	306.27	1	7	6
4	Hesperidin	10621	C <sub>28</sub> H <sub>34</sub> O <sub>15</sub>	610.56	7	15	8
5	Chlorogenic acid	1794427	C <sub>16</sub> H <sub>18</sub> O <sub>9</sub>	354.31	5	9	6
6	Rutin	5280805	C <sub>27</sub> H <sub>30</sub> O <sub>16</sub>	610.52	6	16	10
7	Prunin-Naringenin-7-O-glucosides	92794	C <sub>21</sub> H <sub>22</sub> O <sub>10</sub>	434.39	4	10	6
8	3'-Benzyloxy-5,6,7,4'-tetramethoxyflavone	7020621	C <sub>26</sub> H <sub>24</sub> O <sub>7</sub>	448.46	8	7	0
9	3-Feruloylquinic acid	10133609	C <sub>17</sub> H <sub>20</sub> O <sub>9</sub>	368.34	6	9	5
10	Kaempferitrin	5486199	C <sub>27</sub> H <sub>30</sub> O <sub>14</sub>	578.52	5	14	8
11	Tolrestat*	53359	C <sub>16</sub> H <sub>14</sub> F <sub>3</sub> NO <sub>3</sub> S	357.3	6	6	1
12	Acarbose *	41774	C <sub>25</sub> H <sub>43</sub> NO <sub>18</sub>	645.50	9	19	14

**KEY:** \* denotes the standard drugs incorporated in this study. MF= Molecular formula, MW= Molecular weight, NRB= Number of rotatable bonds, NHBA= Number of hydrogen bond acceptors, and NHBD= Number of hydrogen bond donors.

**Table 5.2.** Lipophilicity and water solubility properties of the top ten ligands

S/N	Ligands	PubChem ID	Log Po/w (iLOGP)	Log S (ESOL)
1	$\beta$ -Sitosterol	222284	5.05	-7.90 (poorly soluble)
2	Genkwanin	5281617	2.48	-4.14 (Moderately soluble)
3	Epigallocatechin	72277	0.98	-2.08 (Soluble)
4	Hesperidin	10621	2.60	-3.28 (Soluble)
5	Chlorogenic acid	1794427	0.96	-1.62 (Very soluble)
6	Rutin	5280805	1.58	-3.30 (Soluble)
7	Prunin-Naringenin-7-O-glucosides	92794	2.38	-2.97 (Soluble)
8	3'-Benzyloxy-5,6,7,4'-tetramethoxyflavone	7020621	4.23	-5.44 (Moderately soluble)
9	3-Feruloylquinic acid	10133609	1.47	-1.84 (Very soluble)
10	Kaempferitrin	5486199	1.89	-3.33 (Soluble)
11	Tolrestat*	53359	2.42	-4.29 (Moderately soluble)
12	Acarbose *	41774	1.43	2.13 (Highly soluble)

**KEY:** \* denotes the standard drugs incorporated in this study

**Table 5.3.** Pharmacokinetic properties of the top ten ligands

<b>Ligands</b>	<b>GI Absorption</b>	<b>BBB Permeant</b>	<b>P-gp Substrate</b>	<b>CYP1A2 Inhibitor</b>	<b>CYP2C19 Inhibitor</b>	<b>CYP2C9 Inhibitor</b>	<b>CYP2D6 Inhibitor</b>	<b>CYP3A4 Inhibitor</b>
$\beta$ -Sitosterol	Low	No	No	No	No	No	No	No
Genkwanin	High	No	No	Yes	No	yes	Yes	Yes
Epigallocatechin	High	No	No	No	No	No	No	No
Hesperidin	Low	No	Yes	No	No	No	No	No
Chlorogenic acid	Low	No	No	No	No	No	No	No
Rutin	Low	No	Yes	No	No	No	No	No
Prunin-Naringenin-7-O-glucosides	Low	No	Yes	No	No	No	No	No
3'-Benzyloxy-5,6,7,4'-tetramethoxy flavone	High	No	Yes	No	Yes	Yes	No	Yes
3-Feruloylquinic acid	Low	No	No	No	No	No	No	No
Kaempferitrin	Low	No	Yes	No	No	No	No	No
Tolrestat*	High	No	No	Yes	Yes	No	No	No
Acarbose*	Low	No	Yes	No	No	No	No	No

**Table 5.4.** Drug-likeness properties of the top ten ligands

SN	Ligands	Lipinski	Ghose	Veber	Egan	Mugge	BS
1.	$\beta$ -Sitosterol	Yes; 1 violation	Yes; 1 violation	Yes	No; 1 violation	No; 2 violations	0.55
2.	Genkwanin	Yes; 0 violation	Yes	Yes	Yes	Yes	0.55
3.	Epigallocatechin	Yes; 1 violation	Yes	Yes	Yes	No; 1 violation	0.55
4.	Hesperidin	No; 3 violations	No; 4 violations	No; 1 violation	No; 1 violation	No; 4 violations	0.17
5.	Chlorogenic acid	Yes; 1 violation	No; 1 violation	No; 1 violation	No; 1 violation	No; 2 violations	0.11
6.	Rutin	No; 3 violations	No; 4 violations	No; 1 violation	No; 1 violation	No; 4 violations	0.17
7.	Prunin-Naringenin-7-O-glucosides	Yes; 1 violation	Yes	No; 1 violation	No; 1 violation	No; 2 violations	0.55
8.	3'-Benzyloxy-5,6,7,4'-tetramethoxy flavone	Yes; 0 violation	Yes	Yes	Yes	Yes	0.55
9.	3-Feruloylquinic acid	Yes; 0 violation	No; 1 violation	No; 1 violation	No; 1 violation	No; 1 violation	0.11
10.	Kaempferitrin	No; 3 violations	No; 4 violations	No; 1 violation	No; 1 violation	No; 3 violations	0.17
	Tolrestat*	Yes; 0 violation	Yes	Yes	Yes	Yes	0.56
	Acarbose*	No; 3 violations	No; 4 violations	No; 1 violation	No; 1 violation	No; 5 violations	0.17

**KEY:** \* denotes the standard drugs incorporated in this study. BS= Bioavailability scores

**Table 5.5.** Medicinal chemistry prediction of the top ten ligands

<b>Ligands</b>	<b>PAINS</b>	<b>Brenk</b>	<b>Leadlikeness</b>	<b>Synthetic availability</b>
β-Sitosterol	0 alert	1 alert: isolated_alkene	No; 2 violations: MW>350, XLOGP3>3.5	6.30
Genkwanin	0 alert	0 alert	Yes	3.03
Epigallocatechin	1 alert: catechol_A	1 alert: catechol	Yes	3.53
Hesperidin	0 alert	0 alert	No; 1 violation: MW>350	6.34
Chlorogenic acid	1 alert: catechol_A	2 alerts: catechol, michael_acceptor_1	No; 1 violation: MW>350	4.16
Rutin	1 alert: catechol_A	1 alert: catechol	No; 1 violation: MW>350	6.52
Prunin-Naringenin-7-O-glucosides	0 alert	0 alert	No; 1 violation: MW>350	4.98
3'-Benzyloxy-5,6,7,4'-tetramethoxy flavone	0 alert	0 alert	No; 3 violations: MW>350, Rotors>7, XLOGP3>3.5	4.05
3-Feruloylquinic acid	0 alert	1 alert: michael_acceptor_1	No; 1 violation: MW>350	4.25
Kaempferitrin	0 alert	0 alert	No; 1 violation: MW>350	6.48
Tolrestat*	0 alert	1 alert: thiocarbonyl_group	No; 2 violations: MW>350, XLOGP3>3.5	2.34
Acarbose*	0 alert	1 alert: isolated_alkene	No; 2 violations: MW>350, Rotors>7	7.34

**KEY:** \* denotes the standard drugs incorporated in this study.

**Table 5.6.** Toxicity prediction of the top ten ligands

<b>Ligands</b>	<b>Carcino-genicity</b>	<b>Hepato-toxicity</b>	<b>Respiratory toxicity</b>	<b>Reproductive toxicity</b>	<b>Mitochondri a toxicity</b>	<b>Nephro toxicity</b>	<b>Acute oral toxicity</b>	<b>PPAR Gamma</b>	<b>Eye irritation</b>	<b>Skin irritation</b>
β-Sitosterol	-	+	+	+	+	-	I	+	-	+
Genkwanin	-	-	-	+	-	-	III	+	+	-
Epigallocatechin	-	+	+	+	+	-	IV	+	+	-
Hesperidin	-	-	-	+	-	-	III	+	-	-
Chlorogenic acid	-	+	+	+	+	-	III	+	-	-
Rutin	-	+	+	+	-	-	III	+	-	-
Prunin-Naringenin-7-O-glucosides	-	-	-	+	+	+	III	+	-	-
3'-Benzyloxy-5,6,7,4'-tetramethoxy flavone	-	-	-	+	-	-	III	+	-	-
3-Feruloylquinic acid	-	+	+	+	+	-	III	-	-	-
Kaempferitrin	-	-	-	+	+	-	III	+	-	-
Tolrestat*	-	+	+	+	+	-	III	+	-	-
Acarbose*	-	+	+	+	+	-	IV	+	-	-

**KEY:** \* denotes Standard drug

+ Denotes active

- Denotes inactive

**I** Denotes highly toxic and highly irritating

**II** Denotes moderately toxic and moderately irritating

**III** Denotes slightly toxic and slightly irritating

**IV** Denotes practically non-toxic and non-irritating

Table 6 presents the effect of *Cucumis sativus* peel extract (CSPE) on both protein concentration and glucose levels. The results indicate that administration of 600 mg of CSPE led to a significant ( $p<0.05$ ) increase in protein concentration, suggesting a potential role in enhancing protein synthesis or preserving structural and functional proteins in diabetic conditions. Conversely, glucose levels were significantly reduced ( $p<0.05$ ) compared to both the control and STZ-untreated diabetic groups, indicating the hypoglycemic potential of CSPE. This reduction in glucose levels may be attributed to improved insulin sensitivity, enhanced glucose uptake by peripheral tissues, or modulation of key metabolic pathways involved in carbohydrate metabolism.

**Table 6.** Effects of CSPE on Protein and Glucose Concentrations

S/N	Experimental Groups	Protein Conc. [mg/ dL]	Glucose Conc. [mg/ mL]
1.	Control	0.25 ± 0.06 <sup>a</sup>	86.15 ± 1.24 <sup>a</sup>
2.	STZ	0.13 ± 0.02 <sup>b</sup>	207.41 ± 4.90 <sup>b</sup>
3.	STZ + CSPE 600 mg	0.29 ± 0.05 <sup>a</sup>	138.30 ± 2.68 <sup>c</sup>
4.	STZ + Glb	0.16 ± 0.03 <sup>b</sup>	79.93 ± 1.05 <sup>a</sup>

Data shows mean ± SEM (n=6) and values with different alphabets (a, b, c) are statistically significant at  $p<0.05$ . STZ = streptozotocin, CSPE = *Cucumis sativus* pulp extract and Glb = Glibenclamide.

Figure 2 shows the effect of CSPE on antioxidant activities. The administration of 600 mg CSPE significantly ( $p<0.05$ ) increased both superoxide dismutase (SOD) and catalase (CAT) activities compared to the STZ-untreated group. This increase suggests an enhanced antioxidant defense system, which may contribute to the reduction of oxidative stress and protection of cellular components from free radical damage. Figure 3 shows the effect of CSPE on Liver function parameters. The administration of 600 mg CSPE was observed to significantly ( $p<0.05$ ) decrease both aspartate transferase (AST) and alanine transferase (ALT) activities compared to the STZ-untreated group. This reduction indicates a protective effect on liver tissues, potentially preventing hepatocellular injury and improving overall liver function in diabetic conditions.

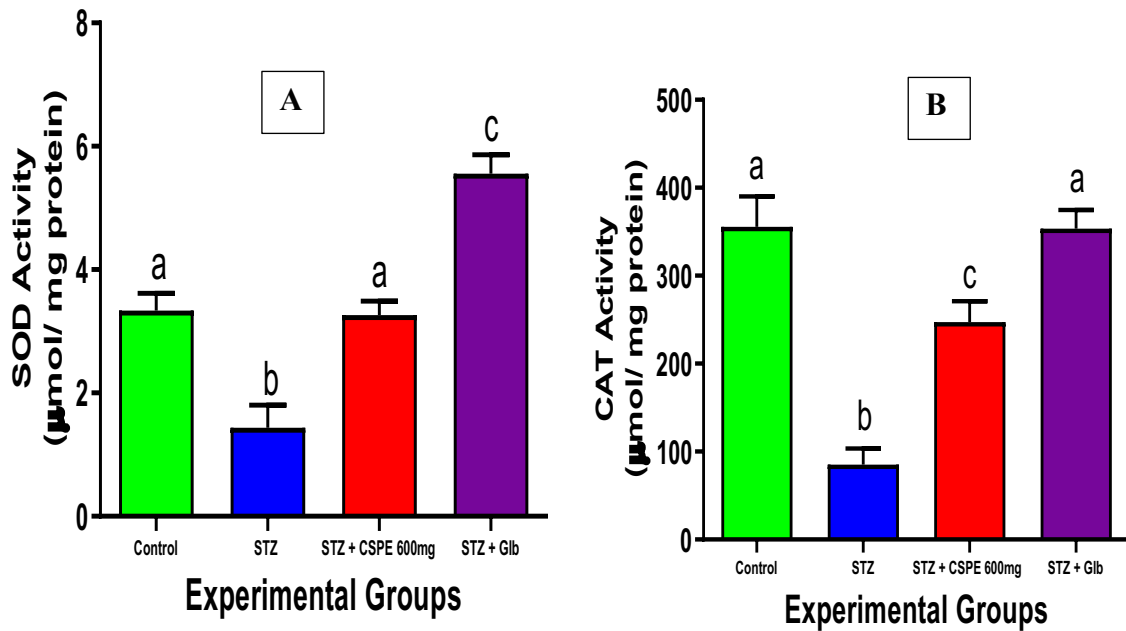


**Figure 2.** Effect of *Cucumis sativus* pulp extract (CSPE) on antioxidant activities in STZ-induced diabetic Wistar rats. Each bar represents mean  $\pm$  SEM (n=6) and bars with different alphabets (a, b, c) are statistically significant at  $p < 0.05$ . STZ = streptozotocin, CSPE = *Cucumis sativus* pulp extract and Glb = Glibenclamide.

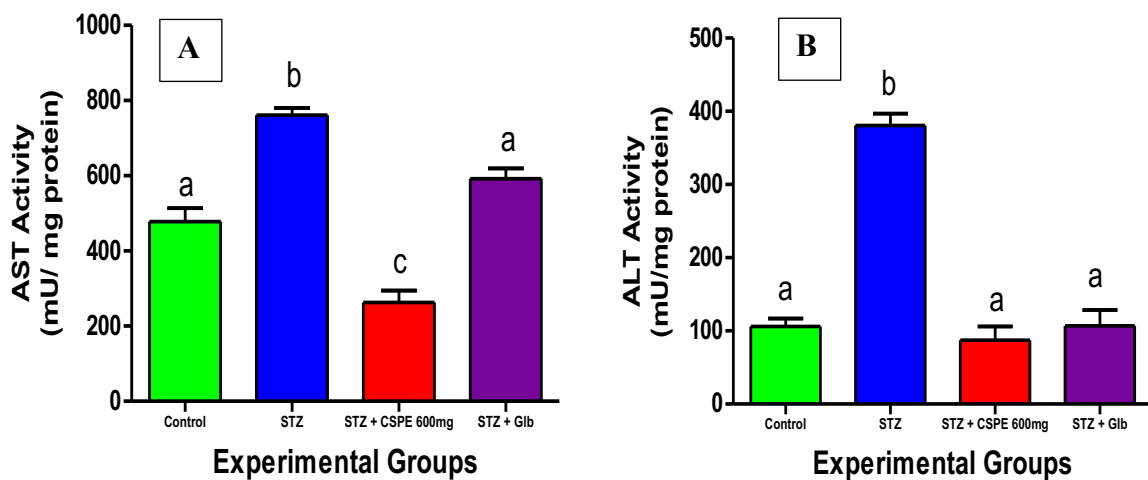


**Figure 3.** Effect of *Cucumis sativus* Pulp Extract (CSPE) on Lipid enzyme activities in STZ-induced diabetic Wistar rats. Each bar represents mean  $\pm$  SEM (n=6) and bars with different alphabets (a, b, c) are statistically significant at  $p < 0.05$ . STZ = streptozotocin, CSPE = *Cucumis sativus* Pulp Extract and Glb = Glibenclamide.

Table 7 presents the effect of *Cucumis sativus* peel extract (CSPE) on oxidative stress markers. The results indicate that the administration of 600 mg of CSPE led to a significant ( $p < 0.05$ ) increase in non-protein thiol (glutathione) concentration compared to the control and STZ-untreated groups. Glutathione plays a crucial role in cellular antioxidant defense by neutralizing reactive oxygen species (ROS) and detoxifying harmful compounds, suggesting that CSPE may enhance endogenous antioxidant capacity.

Furthermore, the administration of 600 mg of CSPE significantly ( $p < 0.05$ ) decreased the concentrations of hydrogen peroxide ( $H_2O_2$ ) and malondialdehyde (MDA) compared to both the control and STZ-untreated groups. The reduction in  $H_2O_2$  levels indicates a lower presence of oxidative radicals that could otherwise contribute to cellular damage. Similarly, the decrease in MDA, a well-known marker of lipid peroxidation, suggests that CSPE helps protect membrane lipids from oxidative degradation, thereby preserving cellular integrity and reducing oxidative damage in diabetic conditions.

However, treatment with 600 mg of CSPE did not result in a statistically significant difference ( $p > 0.05$ ) in nitric oxide (NO) levels when compared to the STZ-untreated group. This finding suggests that while CSPE effectively modulates several oxidative stress markers, its impact on NO metabolism may be limited or require a different dosage or duration of treatment to produce noticeable changes. Nitric oxide plays a dual role in oxidative stress, acting as both a signaling molecule and a potential contributor to oxidative damage, depending on its concentration and interaction with other reactive species. Overall, these findings highlight the potential of CSPE in mitigating oxidative stress by enhancing antioxidant defense mechanisms and reducing lipid peroxidation, which may contribute to its protective role in diabetes management.

**Table 7.** Effects of CSPE on Oxidative stress indices.

S/N	Experimental Groups	$H_2O_2$ [mmol/ mL]	NO [mmol/ mL]	MDA [nmol]	GSH [ $\mu$ mol/ mg protein]
1.	Control	$0.059 \pm 0.01^a$	$0.337 \pm 0.00^a$	$80.02 \pm 2.75^a$	$339.8 \pm 13.78^a$
2.	STZ	$0.194 \pm 0.04^b$	$0.584 \pm 0.31^b$	$297.4 \pm 6.87^b$	$191.6 \pm 7.02^b$
3.	STZ + CSPE 600 mg	$0.081 \pm 0.01^a$	$0.545 \pm 0.44^b$	$132.86 \pm 5.91^c$	$411.5 \pm 23.17^c$
4.	STZ + Glb	$0.076 \pm 0.00^a$	$0.312 \pm 0.05^a$	$108.44 \pm 2.12^c$	$302.5 \pm 6.830^a$

Data shows mean  $\pm$  SEM (n= 6) and values with different alphabets (a, b, c) in the same column are statistically significant at  $p < 0.05$ . STZ = streptozotocin, CSPE = *Cucumis sativus* pulp extract and Glb = Glibenclamide.

Table 8 presents the effect of CSPE on lipid profile indices. The administration of 600 mg of CSPE resulted in a significant ( $p < 0.05$ ) reduction in total cholesterol, triglycerides, low-density lipoprotein cholesterol (LDL-C), and very-low-density lipoprotein cholesterol (VLDL-C) concentrations compared to the STZ-untreated diabetic animals. This suggests that CSPE may play a beneficial role in lipid metabolism by lowering harmful lipids that are commonly elevated in diabetic dyslipidemia, thereby potentially reducing the risk of cardiovascular complications associated with diabetes.

Interestingly, the administration of CSPE resulted in a statistically significant ( $p < 0.05$ ) increase in high-density lipoprotein cholesterol (HDL-C) levels compared to the STZ-untreated diabetic animals. Moreover, there was no statistical significance ( $p > 0.05$ ) between the animals treated with the extract or standard drug, glibenclamide. However, the treated groups were statistically significantly ( $p < 0.05$ ) lower than the normal control. This may indicate that CSPE may help improve lipid profile balance by targeting elevated cholesterol and triglyceride levels. HDL-C

is considered beneficial and good cholesterol as it facilitates reverse cholesterol transport and protects against atherosclerosis. This suggests that while CSPE effectively modulates harmful lipid fractions, it does not significantly enhance protective lipoproteins within the dosage and duration of treatment used in this study.

**Table 8.** Effects of CSPE on Lipid profile indices

S/N	Experimental Groups	Total-Chol [mg/ dL]	TRIG [mg/ dL]	HDL-Chol [mg/ dL]	LDL-Chol [mg/ dL]	VLDL-Chol [mg/dL]
1.	Control	202.6 ± 1.13 <sup>a</sup>	196.2 ± 2.79 <sup>a</sup>	211.4 ± 9.90 <sup>a</sup>	41.77 ± 0.29 <sup>a</sup>	39.24 ± 0.56 <sup>a</sup>
2.	STZ	599.2±0.376 <sup>b</sup>	452.6 ± 39.18 <sup>b</sup>	59.0 ± 0.84 <sup>b</sup>	148.2 ± 11.28 <sup>b</sup>	148.5±9.84 <sup>b</sup>
3.	STZ + CSPE 600 mg	196.4 ± 1.32 <sup>a</sup>	287.4 ± 36.45 <sup>c</sup>	145.04 ± 0.16 <sup>c</sup>	39.95 ± 7.71 <sup>a</sup>	57.48±7.29 <sup>a</sup>
4.	STZ + Glb	295.2 ± 5.755 <sup>c</sup>	237.8 ± 14.07 <sup>a</sup>	167.1 ± 5.725 <sup>c</sup>	55.58 ± 2.64 <sup>a</sup>	50.63±2.27 <sup>a</sup>

Data shows mean ± SEM (n=6) and values with different alphabets (a, b, c) in the same column are statistically significant at  $p < 0.05$ . STZ = streptozotocin, CSPE = *Cucumis sativus* pulp extract and Glb = Glibenclamide.

## Discussion

The choice of 600 mg/kg body weight of *Cucumis sativus* pulp extract used in this study was based on the yield obtained from the extract preparation process and also from a previous study by Saidu *et al.* (2014), who used 500 mg/kg body weight of methanol fruit pulp extract of *C. sativus* for the treatment of alloxan-induced diabetic rats (AIDRs). Meanwhile, the dose of glibenclamide (5 mg/kg body weight) used in this study was based on the dose of each tablet consumed by diabetic patients according to the manufacturer's prescription. Bioactive compounds, including flavonoids, phenolics, tannins, and saponins, were present and abundant in CSPE. These substances have all been linked to glucose and lipid-lowering activities and considerable antioxidant potential (Oloruntoba and Ayodele, 2022). This study showed abundant total flavonoids (TFC), total phenols (TPC), and total tannins (TTC), which are known to scavenge free radicals and reduce oxidative stress, a major contributor to diabetes complications (Quranayati *et al.*, 2023). HPLC further validated the polyphenolic content of CSPE, and their capacities to control glucose metabolism, reduce oxidative stress, and scavenge free radicals have been reported (Chaudhary *et al.* 2023). Various volatile compounds were also observed via GC-MS analysis, and compounds such as sterols, fatty acid compounds, glycosides, and terpenoids were detected. Terpenoids are known to have lipid-lowering properties, hence, the presence of steroids and terpenoids implies that these compounds may be involved in regulating lipid metabolism (Mannino *et al.*, 2021). These comprehensive analyses suggest that *Cucumis sativus* may affect glucose and lipid metabolism.

The induction of diabetes (type 2) with 60 mg/kg body weight of STZ resulted in partial pancreatic failure, but treatment with *Cucumis sativus* pulp extract (CSPE) significantly ( $p < 0.05$ ) reduced and increased the blood glucose and protein concentrations, respectively, compared to STZ-untreated diabetic animals. Since the glucose is only reduced in the treated animals, it is justifiable and appropriate to associate this activity with the fruit's embedded phytochemicals, especially the high polyphenolic content. These polyphenolics may have resulted in improved insulin sensitivity, glucose utilization and metabolic functioning, and overall cell health, respectively, in the treated rats. These findings corroborate the report of

Thabti *et al.* (2012), who suggested that phenolics and flavonoids have blood sugar-lowering bioactivity.

Antioxidant enzymes (SOD and CAT) regulate oxygen and hydrogen peroxide levels by neutralizing radicals and organic peroxides caused by STZ exposure. In this study, STZ-induced diabetes impaired hepatic antioxidant enzymes, with SOD converting superoxide radicals to H<sub>2</sub>O<sub>2</sub> and O<sub>2</sub>, while CAT removes H<sub>2</sub>O<sub>2</sub> (Drabińska, 2024). The reduced liver SOD and CAT activities observed in diabetic animals may result from increased ROS generation, including superoxide (O<sub>2</sub><sup>-</sup>) and hydroxyl (OH<sup>-</sup>) radicals, induced by STZ. These free radicals may have inactivated these enzymes, weakening antioxidant defenses against ROS damage. However, the treatment of the STZ-induced diabetic animals with CSPE significantly ( $p < 0.05$ ) increased the activities of these antioxidant enzymes. In contrast, hydrogen peroxide (H<sub>2</sub>O<sub>2</sub>) and malondialdehyde (MDA) levels significantly ( $p < 0.05$ ) decreased, reflecting reduced oxidative stress. Furthermore, treatment with CSPE significantly ( $p < 0.05$ ) increased non-protein thiol (GSH) concentrations, reinforcing the defense against oxidative stress. These findings may indicate that *Cucumis sativus* fruit pulp extract may help reduce oxidative stress, a critical factor in the progression of diabetes complications (Heidari *et al.*, 2016).

In diabetic conditions, the elevated activities of liver function markers such as aspartate aminotransferase (AST) and alanine aminotransferase (ALT) have been associated with liver dysfunction leading to liver necrosis (Farid *et al.*, 2022). As a result, the increase in serum AST and ALT activity in diabetic untreated control animals may be attributed to the leakages of these enzymes from the liver cytosol into the bloodstream, indicating the hepatotoxic action of STZ.

Conversely, administration of CSPE to the STZ-induced diabetic animals reduced the activity of these enzymes compared to the STZ-induced untreated animals (Mbatha *et al.*, 2022).

In addition to a significant increase in the animal's blood glucose (hyperglycemia) and liver enzyme dysfunction observed following the induction of diabetes using STZ, a significant ( $p < 0.05$ ) increase in lipids (hyperlipidemia) was also observed in the STZ-induced diabetic animals. This is in agreement with the report of Nabi *et al.* (2013). However, treatment with CSPE regulated the lipid profile by significantly ( $p < 0.05$ ) reducing the total cholesterol, triglycerides, LDL-cholesterol, and VLDL-cholesterol levels. Meanwhile, a significant ( $p < 0.05$ ) increase in HDL-cholesterol was observed with the treatment with CSPE. A similar trend has been reported by Al-Snafi *et al.* (2019).

The *in-silico* study provided more insight into the molecular mechanism of *Cucumis sativus* bioactive compounds and the selected diabetes-related protein targets. Molecular docking is an essential computational tool in the field of drug discovery and development for comprehending the interactions that occur between small molecules and target proteins (Sahu *et al.*, 2024). From all the ligands (bioactive compounds) generated from GC-MS and HPLC analyses of *C. sativus*,  $\beta$ -sitosterol and hesperidin showed stronger binding affinities for  $\alpha$ -amylase,  $\alpha$ -glucosidase, sorbitol dehydrogenase, and aldose reductase than the standard drugs incorporated in this study (acarbose and tolrestat). These enzymes (protein targets) are essential for the regulation of insulin and the metabolism of carbohydrates (Dubey *et al.*, 2020), and inhibiting them can decrease blood glucose and increase insulin sensitivity like that of current anti-diabetic medications (Bhosale *et al.*, 2024).  $\beta$ -sitosterol showed the strongest inhibitory effect against  $\alpha$ -amylase and aldose reductase, and hesperidin showed the best affinity for  $\alpha$ -glucosidase and sorbitol dehydrogenase, indicating that the two ligands can regulate or manage diabetes mellitus through these enzymes.

In the last decade, drug failures due to poor pharmacokinetic profiles, medicinal chemistry properties, efficacy, unmanaged toxicity, and inadequate drug-like properties have been on the rise. This led to a focus on improving the drug development process by utilizing ADMET properties at the early stages (Dulsat *et al.*, 2023). In this study, the ADMET properties of the top ten (10) ligands resulting from the *in-silico* study were analyzed using SwissADME, admetSAR, and ProTox software. The physicochemical properties of the top ten (10) ligands showed that  $\beta$ -sitosterol obeyed the Lipinski rule of five while hesperidin disobeyed it (Lipinski, 2004), which shows that all ten ligands have the potential to be used in the development of new pharmaceuticals (Ivanović *et al.*, 2020).

The assessment of the water-soluble properties showed that the ligand with the best binding affinity,  $\beta$ -sitosterol, is poorly soluble in water, meanwhile, its lipophilicity property showed the best solubility in lipids with a value of 5.05 and this may be advantageous because drug potency and lipid solubility improve as the values move away from zero. This aligns with similar studies by Chmiel *et al.* (2019). The evaluation of the drug-likeness properties showed that the top ten ligands had good bioavailability scores of 0.55, which is encouraging because a chemical must have a bioavailability score of at least 0.10 to be classified as a drug candidate (Ntie-Kang *et al.*, 2019; Awote *et al.*, 2024). Three of the top ten ligands – epigallocatechin, chlorogenic acid, and rutin showed positive pan-assay interference compounds (PAINS) indication. Meanwhile, genkwanin and epigallocatechin showed lead-like indications. Furthermore, all the best ten ligands and the standard drugs have a synthetic score ranging from

2.34 to 7.34, where acarbose demonstrated the best synthetic accessibility. This may imply that this compound can be easily used in the synthesis of a new drug (Stratton *et al.*, 2015). The blood-brain barrier permeability showed a negative indication for all the ligands, as a result, this compound may not be developed for use in the treatment of central nervous system (CNS) disorders, especially in neurological disorders, including dementia, schizophrenia, and Alzheimer's disease (Małkiewicz *et al.*, 2019). SwissADME and admetSAR predictions revealed that all of the top ten ligands have a negative indicator for carcinogenic toxicity and a positive indicator for reproductive toxicity. Seven compounds, including  $\beta$ -sitosterol, epigallocatechin, chlorogenic acid, rutin, tolrestat, acarbose, and 3-feruloylquinic acid, showed a positive indicator for hepatotoxicity and respiratory toxicity. In addition,  $\beta$ -sitosterol, epigallocatechin, chlorogenic acid, prunin-naringenin-7-O-glucosides, acarbose, tolrestat, and 3-feruloylquinic acid predicted mitochondrial toxicity, while prunin-naringenin-7-O-glucosides predicted nephrotoxicity.

## Conclusion

In conclusion, the findings from this study suggest *Cucumis sativus* fruit as a functional food with possible natural medicinal therapeutic properties for the management and treatment of diabetes, particularly in reducing oxidative stress, improving liver function, and regulating glucose and lipid metabolism. Additionally, its antioxidant properties likely play a crucial role in protecting pancreatic and hepatic tissues from oxidative damage, thereby supporting overall metabolic health.

While these results demonstrate promising antidiabetic effects, further studies are required to isolate and characterize the active phytochemicals responsible for these effects, elucidate their precise molecular mechanisms, and evaluate their long-term safety and efficacy through clinical trials. Future research should also explore the potential synergistic effects of *Cucumis sativus* with existing antidiabetic medications and its application in functional food formulations. These insights could contribute to the development of novel nutraceutical strategies for diabetes

prevention and management.

### Declaration of Conflict of Interest

The authors of this research declare no known financial or any other conflict of interest.

### Authors and Contribution

O.K.A. developed the concept and designed experiments. B.O.O. carried out the investigation and wrote the first draft. A.G.A. conducted the *in-silico* bioinformatics analyses. I.O.A. performed the statistical analysis. O.O.O. and B.D.K. reviewed and edited the manuscript.

### References

- Adamu, A. U., Abdulmumin, Y., & Mustapha, R. K. (2021). Green Synthesis, Characterization and Phytochemicals Analysis of Silver Nano-Particles Using Aqueous Peel Extract of *Cucumis sativus*. *J. Mater. Environ. Sci*, 12(12), 1627-1636.
- Andrés, C. M. C., Lastra, J. M. P. D. L., Juan, C. A., Plou, F. J., & Pérez-Lebeña, E. (2023). Chemical insights into oxidative and nitrative modifications of DNA. *International Journal of Molecular Sciences*, 24(20), 15240.
- Andrés, C. M. C., Pérez de la Lastra, J. M., Juan, C. A., Plou, F. J., & Pérez-Lebeña, E. (2024). Antioxidant Metabolism Pathways in Vitamins, Polyphenols, and Selenium: Parallels and Divergences. *International Journal of Molecular Sciences*, 25(5), 2600.
- Afzal, S., Abdul Manap, A. S., Attiq, A., Albokhadaim, I., Kandeel, M., & Alhojaily, S. M. (2023). From imbalance to impairment: the central role of reactive oxygen species in oxidative stress-induced disorders and therapeutic exploration. *Frontiers in Pharmacology*, 14, 1269581.
- Awote OK, Amisu KO, Anagun OS, Dohou FP, Olokunola ER and Elum NO. (2024). *In vitro* and Molecular Docking Evaluation of the Antibacterial, Antioxidant, and Antidiabetic Effects of Silver Nanoparticles from *Cymbopogon citratus* Leaf. *Tropical Journal of Natural Product Research (TJNPR)*, 8(9): 8400–8411.
- Awote, O.K., Kazeem, M.I., Ojekale, A.B., Ayanleye, O.B., & Ramoni, H.T. (2023). Prospects of silver nanoparticles (AgNPs) synthesized by *Justicia secunda* aqueous extracts on diabetes and its related complications. *Proc Nig Acad Sci.*, 16(1): 87-105.
- Awote, O.K., Apete, S.K., Igbalaye, J.O., Adeyemo, A.G., Dele-osedele, P.I., Thomas-Akinwale, K., Boniwey, T.S., Ogunbamowo, A.A., Ebube, S.C., Folami, S.O. (2022). Phytochemical Screening, Antioxidant, and  $\alpha$ -Amylase Inhibitory Activities of *Acacia nilotica* Seed Methanol Extract. *Adv J Curr Res.*, 7(8): 1-27.
- Awote, O. K., Igbalaye, J. O., & Gideon, A. (2021). Effect of *Phragmanthera incana* Leaves Extracts on Lipid Profile in Wistar Rats Fed High-Fat Diet. *International Journal of Formal Sciences: Current and Future Research Trends*, 12(1), 23-32.
- Banu, S., & Bhowmick, A. (2017). Therapeutic targets of type 2 diabetes: An overview. *MOJ Drug Des. Dev. Ther*, 1(11).

- Bhosale, H. J., Mamdapure, S. V., Panchal, R. B., & Dhuldhaj, U. P. (2024).  $\alpha$ -Amylase,  $\alpha$ -glucosidase, and aldose reductase inhibitory and molecular docking studies on *Tinospora cordifolia* (Guduchi) leaf extract. *Future Journal of Pharmaceutical Sciences*, 10(1), 107.
- Chaudhary, P., Janmeda, P., Docea, A. O., Yeskaliyeva, B., Abdull Razis, A. F., Modu, B., Calina, D., & Sharifi-Rad, J. (2023). Oxidative stress, free radicals and antioxidants: Potential crosstalk in the pathophysiology of human diseases. *Frontiers in chemistry*, 11, 1158198.
- Chmiel, T., Mieszkowska, A., Kempieńska-Kupczyk, D., Kot-Wasik, A., Namieśnik, J., & Mazerska, Z. (2019). The impact of lipophilicity on environmental processes, drug delivery and bioavailability of food components. *Microchemical Journal*, 146, 393-406.
- Daliri, E. B. M., Oh, D. H., & Lee, B. H. (2017). Bioactive peptides. *Foods*, 6(5), 32. Drabińska, N. (2024). Current Perspective About the Effect of a Ketogenic Diet on Oxidative Stress—a Review. *Polish Journal of Food and Nutrition Sciences*, 74(1), 92-105.
- Dubey, K., Dubey, R., Gupta, R., & Gupta, A. K. (2020).  $\alpha$ -Amylase,  $\alpha$ -Glucosidase and Aldose reductase Inhibitory Potential of Betanin for the Management of Diabetes and its complications. *Journal of Advanced Scientific Research*, 11(03), 92-95.
- Dulsat, J., López-Nieto, B., Estrada-Tejedor, R., & Borrell, J. I. (2023). Evaluation of free online ADMET tools for academic or small biotech environments. *Molecules*, 28(2), 776.
- Farid, M. M., Aboul Naser, A. F., Salem, M. M., Ahmed, Y. R., Emam, M., & Hamed, M. A. (2022). Chemical compositions of *Commiphora opobalsamum* stem bark to alleviate liver complications in streptozotocin-induced diabetes in rats: Role of oxidative stress and DNA damage. *Biomarkers*, 27(7), 671-683.
- Green, L. C., Wagner, D. A., Glogowski, J., Skipper, P. L., Wishnok, J. S., & Tannenbaum, S. R. (1982). Analysis of nitrate, nitrite, and [<sup>15</sup>N] nitrate in biological fluids. *Analytical biochemistry*, 126(1), 131-138.
- Haghani, F., Arabnezhad, M. R., Mohammadi, S., & Ghaffarian-Bahraman, A. (2022). Aloe vera and streptozotocin-induced diabetes mellitus. *Revista Brasileira de Farmacognosia*, 32(2), 174-187.
- Heidari, H., Kamalinejad, M., & Eskandari, M. R. (2012). Hepatoprotective activity of *Cucumis sativus* against cumene hydroperoxide induced-oxidative stress. *Research in Pharmaceutical Sciences*, 7(5), 936.
- Hossain, M. J., Al-Mamun, M., & Islam, M. R. (2024). Diabetes mellitus, the fastest growing global public health concern: Early detection should be focused. *Health Science Reports*, 7(3), e2004.
- Ivanović, V., Rančić, M., Arsić, B., & Pavlović, A. (2020). Lipinski's rule of five, famous extensions and famous exceptions. *Popular Scientific Article*, 3(1), 171-177.

- Jollow, D. J., Mitchell, J. R., Zampaglione, N. A., & Gillette, J. R. (1974). Bromobenzene-induced liver necrosis. Protective role of glutathione and evidence for 3, 4-bromobenzene oxide as the hepatotoxic metabolite. *Pharmacology*, 11(3): 151-169.
- Khan, A., Mishra, A., Hasan, S. M., Usmani, A., Ubaid, M., Khan, N., & Saidurrahman, M. (2022). Biological and medicinal application of *Cucumis sativus* Linn.—review of current status with future possibilities. *Journal of Complementary and Integrative Medicine*, 19(4), 843-854.
- Kulkarni, A., Thool, A. R., & Daigavane, S. (2024). Understanding the Clinical Relationship Between Diabetic Retinopathy, Nephropathy, and Neuropathy: A Comprehensive Review. *Cureus*, 16(3):e56674.
- Latha, P. S., Sangeetha, S., Vijayakarthykeyan, M., & Shankar, R. (2024). Prevalence and influencing factors of metabolic syndrome among rural adult population in a district of South India. *Journal of Family Medicine and Primary Care*, 13(8), 3122-3128.
- Lipinski, CA. (2004). Lead-and drug-like compounds: the rule-of-five revolution. *Drug Discovery Today: Technologies*, 1(4): 337-41.
- Lowry, O.H., Rosebrough, N.J., Farr, A.L., Randall, R.J., 1951. Protein measurement with the Folin phenol reagent. *Journal of Biological Chemistry*, 193: 265–275
- Magliano, D. J., & Boyko, E. J. (2022). IDF diabetes atlas.
- Małkiewicz, M. A., Szarmach, A., Sabisz, A., Cubala, W. J., Szurowska, E., & Winklewski, P. J. (2019). Blood-brain barrier permeability and physical exercise. *Journal of neuroinflammation*, 16, 1-16.
- Mannino, G., Iovino, P., Lauria, A., Genova, T., Asteggiano, A., Notarbartolo, M., Porcu, A., Serio, G., Chinigò, G., Occhipinti, A. and Capuzzo, A., Medana, C., Munaron, L., & Gentile, C. (2021). Bioactive triterpenes of *Protium heptaphyllum* gum resin extract display cholesterol-lowering potential. *International Journal of Molecular Sciences*, 22(5), 2664.
- Mbatha, B., Khathi, A., Sibiya, N., Booysen, I., & Ngubane, P. (2022). A Dioxidovanadium Complex cis-[VO<sub>2</sub> (obz)<sub>2</sub>py] Attenuates Hyperglycemia in Streptozotocin (STZ)-Induced Diabetic Male Sprague-Dawley Rats via Increased GLUT4 and Glycogen Synthase Expression in the Skeletal Muscle. *Evidence-Based Complementary and Alternative Medicine*, 2022(1), 5372103.
- Molly, J., Edison, S., Vijayaraghavan, R., & Ajith, T. A. (2017). Effect of curry leaves and cucumber fruit on lipid profile in menopausal women with hyperlipidemia: a randomized controlled pilot study. *Int J Clin Trials*, 4(1), 7-13.
- Mukai, E., Fujimoto, S., & Inagaki, N. (2022). Role of reactive oxygen species in glucose metabolism disorder in diabetic pancreatic  $\beta$ -cells. *Biomolecules*, 12(9), 1228.
- Ntie-Kang, F., Nyongbela, K. D., Ayimele, G. A., & Shekfeh, S. (2019). “Drug-likeness” properties of natural compounds. *Physical Sciences Reviews*, 4(11), 20180169.

- Ogunyinka, B.I., Oyinloye, B.E., Osunsanmi, F.O., Opoku, A.R., & Kappo, A.P. (2017). Protective effects of *Parkia biglobosa* protein isolate on streptozotocin-induced hepatic damage and oxidative stress in diabetic male rats. *Molecules*, 22(10): 1654.
- Oladimeji, S.O., Soares, A.S., Igbalaye, J.O., Awote, O.K., Adigun, A.K., & Awoyemi, Z.O. (2022). Ethanolic Root Extract of *Urtica dioica* Exhibits Pro-fertility and Antioxidant Activities in Female Albino Rats. *International Journal of Biochemistry Research & Review*. 31(8):29-38.
- Oladimeji, S.O., Igbalaye, J.O., Awote, O.K., Shodimu, B.O., Oladeinde, D.T., Omorowa, V.T., Oluwole, S.M., Akinyemi, Y.A., Shobowale, A.Y., Jimoh, D., & Balogun, S.T. (2023). *Cissampelos pareira* ethanolic extract modulates hormonal indices, lipid profile, and oxidative parameters in transient infertility-induced female albino rats. *Bio- Research*, 21(2), pp.1961-1972.
- Oloruntola, O. D., & Ayodele, S. O. (2022). Phytochemical, proximate, and mineral composition, antioxidant and antidiabetic properties evaluation and comparison of mistletoe leaves from moringa and kolanut trees. *Turkish journal of agriculture-food science and technology*, 10(8), 1524-1531.
- Padhi, S., Nayak, A. K., & Behera, A. (2020). Type II diabetes mellitus: a review on recent drug-based therapeutics. *Biomedicine & Pharmacotherapy*, 131, 110708.
- Popoviciu, M. S., Paduraru, L., Nutas, R. M., Ujoc, A. M., Yahya, G., Metwally, K., & Cavalu, S. (2023). Diabetes mellitus secondary to endocrine diseases: an update of diagnostic and treatment particularities. *International Journal of Molecular Sciences*, 24(16), 12676.
- Prince, P.S.M., & Menon, V.P., (2003). Hypoglycaemic and hypolipidaemic action of alcohol extract of *Tinospora cordifolia* root in chemical-induced diabetes in rats. *Phytotherapy Research* 17: 410–413.
- Quranayati, Q., Iqhrammullah, M., Saidi, N., Nurliana, N., Idroes, R., & Nasution, R. (2023). Extracts from *Phyllanthus emblica* L stem barks ameliorate blood glucose level and pancreatic and hepatic injuries in streptozotocin-induced diabetic rats. *Arabian Journal of Chemistry*, 16(9), 105082.
- Sahu, M. K., Nayak, A. K., Hailemeskel, B., & Eyupoglu, O. E. (2024). Exploring recent updates on molecular docking: Types, method, application, limitation & future prospects. *International Journal of Pharmaceutical Research and Allied Sciences*, 13(2-2024), 24-40.
- Saidu, A. N., Oibiokpa, F. I., & Olukotun, I. O. (2014). Phytochemical screening and hypoglycemic effect of methanolic fruit pulp extract of *Cucumis sativus* in alloxan-induced diabetic rats. *Journal of Medicinal Plants Research*, 8(39), 1173-1178.
- Sari, T. A., Chandra, B., & Rivai, H. (2021). Overview of traditional use, phytochemical, and pharmacological activities of cucumber (*Cucumis sativus* L.). *International Journal of Pharmaceutical Sciences and Medicine*, 6(3), 39-49.
- Singh, R., Gholipourmalekabadi, M., & Shafikhani, S. H. (2024). Animal models for type 1 and

- type 2 diabetes: advantages and limitations. *Frontiers in Endocrinology*, 15, 1359685.
- Sood, A., Kaur, P., & Gupta, R. (2012). Phytochemical screening and antimicrobial assay of various seeds extract of Cucurbitaceae family.
- Stratton, C. F., Newman, D. J., & Tan, D. S. (2015). Cheminformatic comparison of approved drugs from natural product versus synthetic origins. *Bioorganic & medicinal chemistry letters*, 25(21), 4802-4807.
- Thabti, I., Elfalleh, W., Hannachi, H., Ferchichi, A., & Campos, M. D. G. (2012). Identification and quantification of phenolic acids and flavonol glycosides in Tunisian *Morus* species by HPLC-DAD and HPLC-MS. *Journal of Functional Foods*, 4(1), 367-374.
- Varshney, R., & Kale, R. K. (1990). Effects of calmodulin antagonists on radiation-induced lipid peroxidation in microsomes. *International journal of radiation biology*, 58(5), 733-743.
- Wolff, S.P. (1994). Ferrous ion oxidation in the presence of ferric ion indicator xylenol orange for measurement of hydroperoxides. *Methods in Enzymology*, 233: 182–189.
- World Health Organization. (2019). *Global action plan on physical Activity 2018-2030: More Active People for a healthier world*. World Health Organization.
- Yedjou, C. G., Grigsby, J., Mbemi, A., Nelson, D., Mildort, B., Latinwo, L., & Tchounwou, P. B. (2023). The management of diabetes mellitus using medicinal plants and vitamins. *International Journal of Molecular Sciences*, 24(10), 9085.